HHS Public Access

Author manuscript

*Cell Rep*. Author manuscript; available in PMC 2017 October 30.

Published in final edited form as:

*Cell Rep*. 2017 October 03; 21(1): 208–221. doi:10.1016/j.celrep.2017.09.036.

# Precocious Interleukin 21 Expression in Naïve Mice Identifies a Natural Helper Cell Population in Autoimmune Disease

**Elisabeth A. Marnik**[1,2], **Xulong Wang**[1], **Thomas J. Sproule**[1], **Giljun Park**[1], **Gregory J. Christianson**[1], **Sarah Kate Lane-Reticker**[1], **Shweta Jain**[3], **Theodore Duffy**[1], **Hongsheng Wang**[3], **Gregory W. Carter**[1,2], **Herbert C. Morse III**[3,*], and **Derry C. Roopenian**[1,2,4,*]

[1]The Jackson Laboratory, Bar Harbor, ME, USA

[2]Genetics Program, Sackler School of Graduate Biomedical Sciences, Tufts University, Boston, MA, USA

[3]Virology and Cellular Immunology Section, Laboratory of Immunogenetics, NIAID, NIH, Rockville, MD

## SUMMARY

Interleukin 21 (IL21) plays key roles in humoral immunity and autoimmune diseases. It is known to function in mature $CD4^+$ T follicular B cell helper ($T_{FH}$) cells but its potential involvement in early T cell ontogeny is unclear. Here, we find that a significant population of newly activated thymic and peripheral $CD4^+$ T cells functionally express IL21 soon after birth. This naturally occurring population, termed natural (n)$T_H21$ cells, exhibits considerable similarity to mature $T_{FH}$ cells. n$T_H21$ cells originating and activated in the thymus are strictly dependent on AIRE and express high levels of NUR77 consistent with a bias toward self-reactivity. Their activation/expansion in the periphery requires gut microbiota and is held in check by $FoxP3^+$ $T_{REG}$ cells. n$T_H21$ cells are the major thymic and peripheral populations of $IL21^+$ cells to expand in an IL21-dependent humoral autoimmune disease. These studies link IL21 to T cell ontogeny, self-reactivity and humoral autoimmunity.

## Graphical Abstract

*Correspondence: Contact information: Derry.Roopenian@jax.org, HMORSE@niaid.nih.gov.
[4]Lead Contact

**Accession Numbers**
GSE67171

**Author Contributions**
Conceptualization, D.C.R., H.C.M., G.W.C., and E.A.M.; Methodology, D.C.R., H.C.M., G.W.C., E.A.M and X.W.; Software, G.W.C., and X.W.; Formal Analysis, E.A.M., and X.W.; Investigation, E.A.M, X.W, G.W.C, T.J.S., G.P., G.J.C., S.L.K., T.D. and S.J.; Resources, H.C.M., D.C.R., G.W.C., H.W., and T.D.; Data Curation, X.W., and G.W.C.; Writing – original draft, D.C.R., H.C.M., G.W.C., and E.A.M.; Writing - Review and editing, D.C.R., H.C.M., G.W.C., X.W., H.W., and E.A.M.; Visualization, E.A.M., S.J., and X.W.; Supervision, D.C.R., H.C.M., and G.W.C.; Funding Acquisition, D.C.R., H.C.M., and G.W.C.

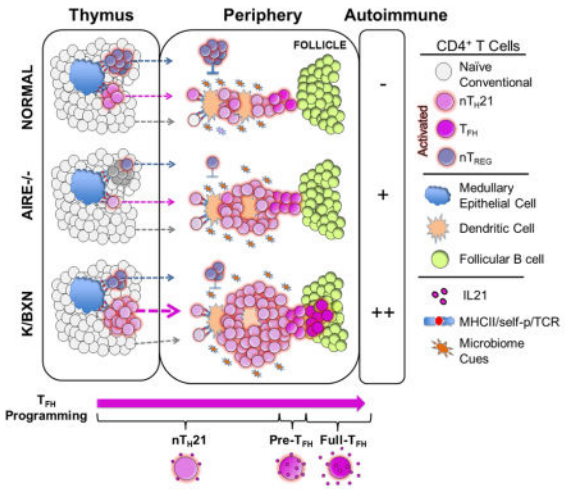


## INTRODUCTION

The helper T ($T_H$) cell cytokine Interleukin 21 (IL21) acting through its broadly expressed receptor, (IL21R), is a critical driver of T-dependent humoral immune responses, supports anti-viral and anti-tumor responses but also promotes autoimmune diseases and the development of lymphomas (Davis et al., 2015; Ettinger et al., 2008; Jain et al., 2015; Spolski and Leonard, 2014). Given the importance of IL21 in health and disease there is need for a deeper understanding of its cellular ontogeny.

Current concepts concerning the cellular ontogeny of IL21 are based largely on studies of adult mice after immunization, infection, or stimulation *in vitro*. Such studies point to $CD4^+$ T follicular B cell helper ($T_{FH}$) cells as the major but not exclusive source of IL21. Prototypical $T_{FH}$ cells express high levels of CXCR5, ICOS and PD1 and localize in B cell follicles where they to help drive antigen-activated B cells to form germinal centers (GCs), affinity mature and differentiate to plasma and memory B cells. This IL21- competent stage is preceded by an IL21-negative, B cell-independent "pre-$T_{FH}$" stage that is characterized by cell surface expression of ICOS and CXCR5 but not PD1 (Barnett et al., 2014; Choi et al., 2011; Crotty, 2014; Goenka et al., 2011). It is initiated when naïve cells are stimulated via their TCRs by antigens presented by DC in a milieu that includes IL6 and ICOS/ICOSL costimulatory factors (Akiba et al., 2005; Barnett et al., 2014; Choi et al., 2011; Crotty, 2014). This directs a transcriptional network governed largely by BCL6 and associated early acting factors that repress alternative $T_H$ fates by limiting expression of BLIMP1 (Choi et al., 2015; Johnston et al., 2009; Liu et al., 2014; Liu et al., 2012; Xu et al., 2015; Yu et al., 2009). This program is reinforced as pre-$T_{FH}$ cells re-encounter cognate antigens as they enter B cell follicles, upregulate CXCR5 and clonally expand as mature $CXCR5^{hi}$ $PD1^+$ $T_{FH}$ and GC $T_{FH}$ cells expressing high levels of IL21. However, residence in B cell follicles may not be absolute as IL21 is expressed by $T_{FH}$-like cells, termed extrafollicular $T_{FH}$ ($_ET_{FH}$) that help extrafollicular B cells differentiate into plasmablasts and contribute to autoimmune diseases (Bubier et al., 2009; Lee et al., 2011; Odegard et al., 2008). Moreover, natural killer T (NKT) cells, $T_H17$ cells and intestinal $CCR9^+$ $CD4^+$ T cells and IFNγ memory $T_H$ cells

can also be sources of IL21 (Coquet et al., 2007; Hsieh et al., 2004; Korn et al., 2009; McGuire et al., 2011; Wei et al., 2007).

As most information on the cellular ontogeny of IL21 is limited to induction and immunization paradigms, we sought here to investigate the potential involvement of IL21 in early stages of T cell development and differentiation in naïve mice. Through use of an IL21 fluorescence reporter mouse, we show that a significant population of $CD4^+$ T cells that are activated in the thymus and periphery soon after birth functionally express IL21. This naturally occurring population, termed natural (n)$T_H21$ cells, exhibits considerable transcriptional overlap with mature $T_{FH}$ cells. n$T_H21$ cells originating in the thymus are strictly dependent on AIRE, express high levels of NUR77 and increase greatly if their TCRs are deliberately biased toward autoreactivity. Their activation/expansion in the periphery is supported by gut microbiota and is held in check by FoxP3 $T_{REG}$ cells. n$T_H21$ cells are also the major thymic and peripheral populations of $IL21^+$ cells to expand in an IL21-dependent humoral autoimmune disease. These studies link IL21 to early stages of T cell ontogeny, self-reactivity and humoral autoimmunity.

## RESULTS

### The IL21-VFP knock-in reliably reports IL21 expression

The IL21-VFP knock-in reporter allele contains an internal ribosomal entry site (IRES)-VFP LoxP-flanked PGK-*Neo*$^R$ selection cassette inserted into the non-coding portion of exon 5 of the mouse *Il21* locus by targeted transgenesis in C57BL6/N (B6)-derived embryonal stem cells (Figures S1A and S1B). Founder mice were crossed to germ-line expressing *cre* mice to genetically excise the *Neo*$^R$ selection cassette. IL21-VFP heterozygotes and homozygotes lacking the selection cassette were born in expected Mendelian ratios and were healthy. There were no alterations in the proportions of splenic lymphocyte subpopulations or the frequencies of naïve cells, spontaneously activated $CD4^+$ $CD44^+$ T cells or $CD4^+$ $ICOS^+$ T cells as determined by flow cytometry, indicating that the reporter did not alter the normal immune status (Figures S1C and data not shown). No differences were noted in the percentages of $VFP^+$ cells between heterozygous and homozygous mice (Figure S1D).

To determine if IL21-VFP reliably reports *Il21* expression *in vitro*, we performed RT-qPCR analysis on FACS-sorted splenic $VFP^+$ and $VFP^-$ $CD4^+$ T cells isolated from IL21-VFP mice after stimulation *in vitro* with anti-CD3/CD28 antibodies. *Il21* and *VFP* transcripts were expressed selectively and at equivalent levels by $VFP^+$ gated cells (Figure S1E). We also found that IL21 was only in supernatants collected from $VFP^+$ $CD4^+$ T cells after they had been stimulated with anti-CD3/CD28 for 36 hrs, sorted, and then cultured independently for 24 hrs. IL21 was accompanied by increased expression of IL2 and IL10. In contrast, IL17 and IFN$\gamma$ were most prominent in supernatants of $VFP^-CD4^+$ T cells (Figure S1F). Thus, VFP accurately reported the transcription and secretion of IL21 by activated $CD4^+$ T cells *in vitro*.

To determine cellular patterns of VFP after immune challenge, IL21-VFP reporter mice were immunized with DNP-KLH. Their splenic and lymph node cells were analyzed 11 days later by flow cytometry. Consistent with VFP expression being limited to $T_{FH}$ and

related cells, a significant fraction of $CD44^+ICOS^+CD4^+$ T cells were $VFP^+$ with many also expressing PD1 (Figure S2A) and approximately 40% of $PD1^+$ cells being $VFP^+$ (Figure S2B). Also notable was the lack of VFP expression by $CD4^+$ T cells expressing the NKT cell marker $NK1.1^+$ and other lymphocyte or leukocyte populations (Figure S2A).

To determine if IL21-VFP reliably reports intracellular IL21, we analyzed splenic $CD4^+$ T cells from 6 wk old B6 mice that were wild type (WT) or heterozygous for IL21-VFP after stimulation with PMA/ionomycin (Figure S2C). VFP (detected by anti-GFP) and intracellular IL21 were expressed concordantly only by activated $CD44^+$ cells with the frequencies of $IL21^+$ cells reduced likely because of lower sensitivity of intracellular IL21 detection (Figure S2C). Similar protocols were used to compare intracellular staining of VFP and IL21 in BXSB.*Yaa* mice whose lupus-like disease is characterized by elevations in $T_{FH}$, $_ET_{FH}$ and IL21 (Bubier et al., 2009). Intracellular VFP and IL21 were coordinately expressed in higher intensities and frequencies by the activated $CD44^+$ population (Figure S2D). To determine the anatomical positioning of IL21-VFP cells, we analyzed $VFP^+$ cells in splenic sections of BXSB.*Yaa* IL21-VFP mice that were in an early stage of disease by immunohistochemistry. Consistent with $T_{FH}$, GC $T_{FH}$ and $_ET_{FH}$ as the sources of IL21, $VFP^+$ T cells were found in B cell follicles, most strongly within $PNA^+$ GC, as well as in T cell zones (Figure S2E). Taken together, the results show that IL21-VFP reliably reports the native patterns of IL21 expression both *in vitro* and *in vivo*.

## Precocious expression of IL21 is a property of an appreciable population of activated peripheral $CD4^+$ T cells that arise postnatally in naïve mice

We then used the IL21-VFP reporter to investigate the patterns of IL21 expression in young naive mice. FACS analysis of spleen cells from 2–4 wk old B6.IL21-VFP mice consistently revealed small populations of $VFP^+$ $CD4^+$ T cells (Figure 1A). Splenic frequencies increased to ~6–7% at 13 wk, paralleled by lower percentages amongst $CD4^+$ T cells in blood at each age (Figure 1B). Essentially all $VFP^+$ cells expressed high levels of the pan-activation marker, CD44, while expression of ICOS and CXCR5 were limited to subpopulations of these cells (Figure 1C). Expression of VFP as measured by mean fluorescence intensity (MFI) did not differ between $ICOS^+$ and $ICOS^-$ cells, but VFP intensities were increased in $CXCR5^+$ cells (Figure 1D). A genetic deficiency in *Cd1d1*, the MHC-like selecting molecule for NKT cells, did not impact the frequencies of $VFP^+$ CD4 T cells indicating that NKT cells were not an appreciable source of IL21 in naive mice (data not shown). We conclude that IL21 expression by $CD4^+CD44^+$ $CXCR5^-$ $PD1^-$ cells is a property of a significant fraction of spontaneously activated, conventional $CD4^+$ T cells that accrue in the periphery of naïve mice within weeks of birth and we term them natural IL21-expressing T helper ($nT_H21$) cells.

We next compared month old reporter mice for the frequencies of $nT_H21$ cells vs. frequencies of cells expressing alternative T-helper cytokines, IFN$\gamma$, IL10, and IL17a, as revealed by age-matched cytokine reporters. In all cases, reporter expression was restricted to splenic $CD4^+$ T cells showing an activated $CD44^+$ phenotype (Figure 1E). $VFP^+$ cells were considerably increased over cells expressing alternative cytokine reporters. Naturally activated (n) $FoxP3^+$ $CD44^+$ $T_{REG}$ cells develop in appreciable frequencies in young naïve

mice (Wyss et al., 2016; Yang et al., 2015). Comparisons of splenic $CD4^+$ T cells from naïve FoxP3-GFP reporter and IL21-VFP mice showed that the frequencies of activated $CD44^+$ $GFP^+$ and $VFP^+$ populations were comparable (Figure 1E). Thus, $nT_H21$ cells are found in the periphery of young, naive mice at frequencies rivaled only by $FoxP3^+$ $nT_{REG}$ cells.

## Cellular, chemokine and cytokine requirements of $nT_H21$ cells

Signals from B cells, ICOS and CXCR5 contribute to the maturation of IL21-competent $T_{FH}$. To determine if such signals are required for $nT_H21$ cells we compared the frequencies of splenic $VFP^+$ cells from naïve *Ighm*$^{-/-}$, *Cxcr5*$^{-/-}$, *Icos*$^{-/-}$ and WT IL21-VFP mice. The lack of B cells or CXCR5 had no significant effect on the frequencies of $VFP^+$ cells (Figures 2A and 2B). However, the MFIs of VFP in mice lacking CXCR5 were lower (Figure 2C). A deficiency in ICOS caused a ~50% reduction in frequency (Figure 2B) but did not affect the VFP MFIs (Figure 2C). Thus, unlike prototypic $T_{FH}$, B cells, ICOS and CXCR5 are not essential for the generation of $nT_H21$ but ICOS increases their frequencies and CXCR5 enhances their expression of IL21.

We then examined the cytokine requirements of $nT_H21$ cells. After crossing the IL21-VFP reporter onto mice homozygous for knockout alleles of *Il6*, *Il10*, *Ifnar1* and *Il21r,* we quantified percentages of splenic $nT_H21$ cells. Mice deficient in IL10 had significantly increased frequencies in $nT_H21$ while a deficiency in IFNAR1 resulted in significant reductions (Figure 2D). Mice lacking IL6 showed minimal reductions, a deficiency in IL21R caused significant reductions, and mice doubly deficient in IL6 and IL21R had the greatest reductions in $nT_H21$ (Figure 2E). Thus, $nT_H21$ are supported by IFN1 and IL21 individually and by IL6 in combination with IL21.

## Comparative RNAseq-based transcriptomics of $nT_H21$ and other naturally arising $CD4^+$ T cell populations

To gain insight into the molecular processes that distinguish $nT_H21$ cells, we performed paired-end mRNAseq on FACS-purified splenic $CD4^+$ T cells from 4 wk old IL21-VFP reporter mice based on the following criteria: naïve $VFP^-$ $ICOS^{lo}$cells (N); activated $VFP^-ICOS^{hi}$ cells (ACT); and $VFP^+$ $ICOS^{int/hi}$ ($nT_H21$) (Figure S3A). Pre-sort analysis indicated that the great majority of $VFP^+$ $ICOS^{int/hi}$ cells were $CXCR5^-/PD1^-$ negative by flow cytometry (Figure S3A–B) but transcriptional elevations of *Cxcr5* and less so for *Pdcd1* (gene for PD1) were detected (Figure S3C). *Icos* and *Cd44* transcripts were similarly upregulated by ACT and $nT_H21$ populations, whereas *Il21* and *VFP* were expressed coordinately and almost exclusively by the gated $nT_H21$ cells (Figure S3C).

We then used hierarchical clustering to evaluate these populations in the context of published microarray datasets of polyclonal mature $T_{FH}$, GC $T_{FH}$, $T_H1$ and naïve cells isolated from mice 8 days after acute infection with lymphocytic choriomeningitis virus (LCMV) (Yusuf et al., 2010) (Figure 3A *top*), and mRNAseq datasets derived from ‘early’ $IL2R\alpha^-Blimp1^-$ $T_{FH}$ and $IL2R\ \alpha^-Blimp1^+$ $T_H1$ cells generated from naïve SMARTA TCR transgenic CD4 T cells adoptively transferred to B6 mice and harvested 3 days after infection with the Armstrong strain of LCMV (Choi et al., 2015) (Figure 3A *bottom*). $nT_H21$

cells clustered closely with $T_{FH}$ generated 3 and 8 days following infection, whereas ACT cells clustered closely with 3 or 8 day $T_H1$ cells.

We then took advantage of our N, ACT and $nT_H21$ datasets to identify groups of genes that most reliably discriminate these populations. We minimized technical noise inherent to low read counts by including only genes having >20 transcripts per million (TPM) in at least one population. Of the 6996 genes meeting these criteria, 471 showed significantly higher expression levels in one subpopulation (Table S1). These included 148 for N; 165 for ACT; and 158 for $nT_H21$ (Figure 3B). Functional gene enrichment analysis of these gene sets using DAVID (https://david.ncifcrf.gov/) showed that $nT_H21$ cells were most enriched for genes associated with T cell development, differentiation, activation, proliferation and adhesion (Figure 3B, Table S2). Thus, $nT_H21$ cells stood out for their transcriptional engagement in T cell activation and signaling processes.

As presented by a 3-way scatterplot (Figure 3C) and gene-selective comparisons (Figures 3D and 3E; Table S3), $nT_H21$ cells were uniquely distinguished by their heightened expression of a number of transcription factors prototypic of $T_{FH}$ cells, including *Ascl2*, *Fosb*, *Pouaf1*, *Tox2*, and *Bcl6,* and low expression of the BLIMP1-encoding gene, *Prdm1*, comparable with N cells. High expression of archetypal $T_{FH}$ markers, including but not limited to *Sostdc1, Btla*, *Cd200*, *Slamf6*, and *Gpm6b,* further supported $T_{FH}$ relatedness. Consistent with a high activation state, $nT_H21$ cells were distinguished by their elevated expression of TCR-related signaling genes, *Lag3, Cd4* and *Cd28*, and a number of cell cycling genes (Figure 3D). $nT_H21$ cells were surprisingly restricted in their effector cytokines; in addition to *Il21*, only *Ifng* was expressed at appreciable levels that were still lower than for the ACT population (Figure 3E). ACT cells, in contrast, were readily distinguished not only by their $T_H1$-relatedness but also by expression patterns consistent with the inclusion of NKT cells, FoxP3 $T_{REG}$, $CCR9^+$ $T_H$, and some $T_H2$ cells (Figure 3E). Expression of key $T_H17$ signature genes, *Rorc*, *Il17a*, and *Il17f,* was minimal in the $nT_H21$ or ACT populations, arguing that few $T_H17$ cells were present (Table S3).

We then mined our RNAseq data to evaluate *Trav* and *Trbv* usage patterns of the naïve (N), activated (ACT) and IL21-ACT ($nT_H21$) populations. ACT showed significant bias, including substantially increased usages of *Trav11* and *Trav11d*, while usages by $nT_H21$ cells did not differ from those of naïve cells (Figure S3C). Taken together, the results show that IL21 expression marks an actively signaling population with diverse TCR usage that is readily distinguished from alternative $CD4^+$ lineages and is equipped with many of the same central transcriptional factors and cell surface receptors of prototypical $T_{FH}$ cells.

## IL6/IL21/BCL6-dependent $nT_H21$ are the major natural T-helper population to develop in the neonatal thymus

The preceding results focused on $nT_H21$ in the periphery. To address the potential thymic ontogeny of $nT_H21$, we performed parallel analyses of thymocytes and splenocytes from WT and naïve IL21-VFP mice at 2 d, 2 wk and 4 wk of age. $VFP^+$ $CD4^+$ $CD8^-$ thymocytes were detected by 2 d and increased to 0.2–0.3% at 2–4 wk with frequencies 5- to 10-fold lower than for their splenic counterparts (Figures 4A and 4B). To determine if the $VFP^+$ thymocytes share cell surface markers with peripheral $nT_H21$, we analyzed both populations

for expression of ICOS, CD44, CD5 and CD3e. Only expression of ICOS was notably different between the thymic and splenic $nT_H21$, with the great majority of thymic $nT_H21$ expressing unusually high levels (Figure 4C). It should be noted that all thymic $VFP^+$ cells are $CD44^+CXCR5^-$ $PD1^-$ and are thus all $nT_H21$ (data not shown). We then addressed their requirements for IL6 and IL21 by comparisons of $nT_H21$ in IL21-VFP mice that were WT or deficient in IL6 and/or IL21R. Only combined deficiencies in IL6 and IL21R resulted in significant reductions of $nT_H21$, consistent with thymic $nT_H21$ being supported by the synergistic effects of IL6 and IL21 (Figure 4D)

We next used fluorescence reporters to compare the proportions of $IL21^+$ $CD4^+$ $CD8^-$ thymocytes with those reporting alternative cytokines (IFN, IL10, IL17) or FoxP3 (Figure 4E). $nT_H21$ cells were the only population found in appreciable frequency by the cytokine reporters, but in lower frequencies than $Foxp3^+$ cells. Thus, and in agreement with patterns found in the periphery, thymic $nT_H21$ cells are a major naturally-activated population exceeded only by thymic $nT_{REG}$ cells.

Given the central role for BCL6 in directing antigen-induced $T_{FH}$ cells (Johnston et al., 2009; Nurieva et al., 2009, Yu et al., 2009; Liu et al., 2012), we used CD4-cre to conditionally delete a *Bcl6*$^{fl}$ allele in IL21-VFP mice. When analyzed at 2 and 6–8 wks of age, $Cre^+$ *Bcl6*$^{fl/fl}$ IL21-VFP mice showed substantial reductions in thymic and splenic frequencies of $nT_H21$ cells compared with CD4-$cre^-$ *Bcl6*$^{fl/lfl}$ littermate and IL21-VFP controls (Figure 4F). Floxing of *Bcl6* did not alter the proportions of double negative, single negative and double positive or activated ($CD44^+$) $CD4^+$ thymocytes (Figure S4). The appreciable reductions of thymic and peripheral $nT_H21$ cells in *Bcl6*-floxed mice are thus consistent with a role for BCL6 in the lineage determination of thymic and peripheral $nT_H21$ cells. Whether the residual $VFP^+$ cells arise from incomplete floxing or BCL6-independence as has been described for $IL21^+$ IFN$\gamma$ memory $T_H$ cells generated after infection with *Plasmodium chabaudi* (Carpio et al., 2015) remains to determined.

## Thymic but not peripheral $nT_H21$ require AIRE and express high levels of Nur77

A primary function of the autoimmune regular, AIRE, is to force the ectopic expression of self-p/MHC molecules not usually encountered in the thymus, including peripheral tissue antigens (PTA), to drive negative selection (Liston et al., 2003). However, recent studies have also uncovered a more nuanced role in which AIRE also safeguards from autoimmunity by diverting the most highly self-reactive thymocytes from conventional T cells to $T_{REG}$ (Kieback et al., 2016; Malchow et al., 2016; Malhotra and Jenkins, 2016). Deficiency in AIRE thus results in the diminution of $nT_{REG}$ capacity and the emergence of self-reactive conventional $CD4^+$ T cells that can inflict systemic autoimmune disease. As thymic $nT_H21$ develop with comparable timing and frequencies to $nT_{REG}$ cells, we determined the effects of AIRE deficiency on their development. The frequencies of $nT_H21$ cells were greatly and equivalently reduced in *Aire*$^{-/-}$ and $^{+/-}$ compared with WT mice suggesting that AIRE controls the thymic development of $nT_H21$ cells in a highly dosage sensitive manner (Figures 5A and 5B). By comparison, in the periphery, AIRE deficiency resulted in a substantial increase in the overall percentages of splenic $VFP^+$ cells and the proportion of activated $CD44^+$ $CD4^+$ cells that were $VFP^+$ (Figures 5B–C). These increases

were predominately in the $nT_H21$ population (Figures 5D). Thus, AIRE supports the thymic development of $nT_H21$ cells but it represses their expansion or generation *de novo* in the periphery.

The strong dependence on AIRE raised the possibility that thymic $nT_H21$ cells are positively selected by strong TCR signals in response to self-p/MHCII ligands, as has been described for thymic $nT_{REG}$ cells (Kieback et al., 2016; Malchow et al., 2016; Malhotra and Jenkins, 2016). Nur77 (encoded by *Nr4a1*) is upregulated immediately after TCR stimulation. Thus, Nur77-GFP transgenic mice provide a convenient means to proxy the strength of TCR/self-p/MHC signaling independent of cytokine induction (Hogquist and Jameson, 2014; Moran and Hogquist, 2012; Qiao et al., 2012). To test if thymic $nT_H21$ cells are actively signaling through their TCRs, we produced Nur77-GFP, IL21-VFP dual reporter mice and used flow cytometry to analyze Nur77-GFP expression by $VFP^+$ and $CD25^+$ $CD4^+$ T cells. Comparison of MFIs of GFP showed that Nur77 was highly expressed by thymic $nT_H21$ cells almost identically to thymic $CD25^+$ $T_{REG}$ cells (Figures 5E and 5 F). However, the MFI of NUR77-GFP for splenic $nT_H21$ cells was reduced to levels comparable to those of naïve cells (Figures 5E and 5F). These results suggest that thymic $nT_H21$ cells are responding strongly to self-p/MHCII signals and to a similar degree as thymic $nT_{REG}$ cells. The reduced expression of Nur77 by $nT_H21$ in the periphery could be due to a dampened need for TCR signaling after thymic exit or by $nT_H21$ that arise *de novo* in the periphery.

## FoxP3$^+$ CD4 T cells and microbial depletion restricts the expansion and maturation of peripheral but not thymic $nT_H21$

As $nT_{REG}$ are potent inhibitors of autoimmunity and are found in young naïve mice at frequencies comparable to thymic and peripheral $nT_H21$ cells, we asked if they restrain $nT_H21$ cells. *Foxp3*-deficient (scurfy) mice are deficient in $nT_{REG}$ cells and consequentially develop severe autoimmune disease within 3–4 wk of birth (Ramsdell and Ziegler, 2014). We generated *Foxp3*$^-$ IL21-VFP reporter mice and analyzed their male progeny at 2 wk of age, when they display few signs of disease, and at 4 wk when they display overt disease. FoxP3 deficiency caused substantial increases in splenic $VFP^+$ cells (Figure 6A) that were primarily $nT_H21$ rather than $CXCR5^+$ $PD1^-$ pre- and CXCR5+ $PD1^+$ full-$T_{FH}$ cells (Figure 6B). The increases in FoxP3-deficient mice were not simply due to global increases in all T-helper subsets because about 40% of $CD44^+$ T cells were $VFP^+$ positive (Figure 6C). However, deficiency in FoxP3 had no significant effect on thymic $nT_H21$ frequencies (Figure 6D). Thus, $nT_H21$ cells that develop in the thymus are insensitive to thymic $nT_{REG}$ cells but are greatly restrained in the periphery by this potent regulatory population.

It has been established that enteric microbiota support the activation and expansion of $T_H$ subsets including $T_{FH}$ (Block et al., 2016; Teng et al., 2016). We therefore addressed the possibility that the expansion of $nT_H21$ in the periphery was influenced by signals from gut microbiota. Cohorts of IL21-VFP mice were treated with ampicillin and sulfatrim in their drinking water starting at 3 wk of age or were left untreated. This treatment resulted in the substantial reduction of fecal bacterial as measured by bacterial16S DNA (Figure 6E). Flow cytometric analyses indicated that antibiotic treatment dramatically reduced the frequencies of splenic $VFP^+$ T cells while not altering the frequencies of thymic $VFP^+$ cells (Figure 6F

and 6G). Thus, stimulatory signals from the gut microbiome support $nT_H21$ cells in the periphery while not affecting those developing in the thymus.

### Peripheral and thymic $nT_H21$ develop in unusually high frequencies in the IL21-dependent K/BXN model of autoimmune arthritis

Given that thymic development of $nT_H21$ cells requires AIRE and constitutes the major $IL21^+$ population to develop in normal and more so in FoxP3 deficient mice, we considered the possibility that heightening their positive selection to self-p/MHC ligands would have disease consequences. TCR transgenic KRN x NOD $F_1$ (K/BXN) mice spontaneously develop autoantibodies against the ubiquitous glycolytic enzyme, glucose 6 phosphate isomerase (GPI), that cause severe arthritis (Korganow et al., 1999; Kouskoff et al., 1996). This humoral autoimmune disease critically requires transgenic $CD4^+$ T cells that are positively selected by the NOD MHC class II molecule $A^{g7}$ to respond strongly to self-GPI/MHCII ligands, and is strictly dependent on IL21 (Block and Huang, 2013; Jang et al., 2009). Its severity also depends on stimulatory cues from enteric bacteria (Block et al., 2016; Wu et al., 2010)

To investigate the possible involvement of $nT_H21$ cells in this strictly IL21-dependent disorder, we produced K/BXN mice carrying the IL21-VFP reporter and characterized their IL21-expressing T cells. Spleens and mesenteric lymph nodes of 10 wk old K/BXN mice showed marked increases in $VFP^+$ cells compared with age-matched IL21-VFP controls, averaging over 37% of $CD4^+$ T cells and 50% of activated $CD44^+$ cells (Figure 7A and 7B). The most striking increase was in $nT_H21$ cells (Figure 7C), although full $T_{FH}$ expressed elevated IL21 as indicated by higher MFIs (Figure 7D). These increases in $VFP^+$ cells were largely negated by antibiotic treatment indicating a key role for gut microbiota (Figure 7E).

We then addressed whether these dynamics were limited to the periphery. Comparison of thymic $VFP^+$ CD4 T cells from K/BXN with control KRN TCR transgene-negative B6xNOD F1 (BXN) IL21-VFP mice showed that K/BXN mice had striking (~10-fold) elevations in thymic $T_H21$ cells as compared with BXN controls in parallel to similar elevations of $VFP^+$ cells in the periphery (Figure 7F–H). Thus, skewing the T cell repertoire toward increased self-reactivity substantially enhanced the thymic selection of $nT_H21$ resulting in abnormally high frequencies of $nT_H21$ and matured $T_{FH}$ populations that depend on microbial stimuli.

## DISCUSSION

Classically, thymocytes with high TCR affinity for self-p/MHC ligands are eliminated, while those with weak but sufficient affinities are positively selected and maintained in the periphery in the naïve state through continued basal self-p/MHC signaling to await immune challenge (Hogquist and Jameson, 2014). However, this paradigm does not account for an assortment of naturally activated $\alpha/\beta$ $CD4^+$ T cell subpopulations found in naïve mice at early age. These include $nT_{REG}$, NKT, $nT_H17$, and intestinal $CCR9^+$ $T_H$ cells and can be further distinguished by their thymic and/or peripheral l origin (Jenkinson et al., 2015; Marks et al., 2009; McGuire et al., 2011; Wyss et al., 2016; Yadav et al., 2013). Through use of a rigorously validated IL21 reporter mouse, we describe a distinct naturally activated

population in which IL21 is functionally expressed and found in surprisingly high frequencies in the thymus and periphery of mice shortly after birth and without deliberate immune challenge.

Transcriptomic analyses provided a glimpse into lineage bifurcations that are established at an early age without immune challenge. Whole transcriptome comparisons of naïve, activated IL21$^{-}$ and IL21$^{+}$ nT$_{H}$21 splenic cells with published data from purified early and mature T$_{FH}$, GC T$_{FH}$ and T$_{H}$1 cell populations induced after viral infection clearly established that nT$_{H}$21 cells were uniquely correlated with early and mature T$_{FH}$ and GC T$_{FH}$ and antithetically to T$_{H}$1 cells. In contrast, the IL21$^{-}$ activated population not only correlated highly with prototypic T$_{H}$1 but also showed transcriptional evidence for alternative naturally-activated populations, including nT$_{REG}$, NKT, and CCR9$^{+}$ T$_{H}$ cells.

nT$_{H}$21 cells stood out in their high expression of an assemblage of markers and cytokines prototypic of T$_{FH}$ and their low expression of genes, including *Prdm1*, indicative of alternative lineages. A T$_{FH}$-like ontogeny was further supported by transcription factors typical of T$_{FH}$ that were specifically increased in nT$_{H}$21 cells, including *Ascl2, Tox2, Fosb, Pou2af1*, *Egr2, Maf* and *E2f2 and Bcl6*. However, some T$_{FH}$-associated transcription factors, including *Lef1*, *Ifr4*, *Batf*, were unchanged or minimally discriminated nT$_{H}$21 from activated IL21$^{-}$ cells. Moreover, the expression patterns of *FoxO1* and *FoxP3,* that are considered to act early on to repress antigen-induced T$_{FH}$ cells by negative regulation of BCL6 and IL21, respectively (Stone et al., 2015; Wang et al., 2014; Weber et al., 2015), were not consistent with their repression of nT$_{H}$21 development or IL21 expression. We suggest that nT$_{H}$21 is an early stage in T$_{FH}$ ontology that is distinguished from alternative naturally activated populations by much of the transcriptional machinery that specifies prototypical T$_{FH}$ cells.

nT$_{H}$21 being an early stage of T$_{FH}$ ontology is further supported by gene knockout studies. According to concepts based on immunization paradigms in adult mice, T$_{FH}$ programming is initiated by encounter with antigen-presenting DC. This pre-T$_{FH}$ stage is characterized by the upregulation of BCL6 and cell surface expression of ICOS and CXCR5 without expression of IL21 (Akiba et al., 2005; Barnett et al., 2014; Choi et al., 2011; Crotty, 2014; Goenka et al., 2011). Similar to previously described pre-T$_{FH}$, we found that nT$_{H}$21 cell development is largely dependent on BCL6 and is unimpaired in B cell-deficient mice. However, nT$_{H}$21 cells differed in that ICOS and CXCR5 were not required for IL21 expression. A genetic deficiency in ICOS resulted in a 50% reduction in nT$_{H}$21 but not lower IL21 expression. A deficiency in CXCR5, in contrast, lowered IL21 expression but did not affect the overall frequencies of nT$_{H}$21 cells. Thus, programming of nT$_{H}$21 cells likely initiates when naïve cells are first activated by DC and receive early inductive signals from BCL6 and to a lesser extent ICOS. This results in nT$_{H}$21 cells expressing IL21 independent of ICOS or CXCR5 signals but with heightened expression in those that have matured to CXCR5$^{+}$ pre-T$_{FH}$ cells.

Our study of mice lacking IFN1, IL10, IL6 and IL21 signals is also consistent with T$_{FH}$-relatedness of nT$_{H}$21 cells while also documenting the tonic effects of these cytokines in young naïve mice. IFN1 signaling in DC stimulates T$_{FH}$ (Cucak et al., 2009) although IFN1

represses $T_{FH}$ cells and IL21 expression after viral infections (Nakayamada et al., 2014; Ray et al., 2014). We found that tonic IFN1 supports $nT_H21$ which may suggest its role in DC conditioning. We also found that $nT_H21$ cells are suppressed by IL10, which is in agreement with its suppression of $T_{FH}$ (Cai et al., 2012). IL6 supports prototypical $T_{FH}$ cells throughout their development and maturation and acts synergistically for IL21 at later stages (Eto et al., 2011). Consistent with synergy of IL6 and IL21, we found that a double deficiency in IL21R and IL6 substantially lowered the frequencies of $nT_H21$ cells. Moreover, the fact that an IL21R deficiency reduced thymic and peripheral $nT_H21$ cells provides strong evidence that IL21 is secreted and functionally consequential in both anatomical locations. Whether IL21 supports $nT_H21$ directly through autocrine feedback (Nurieva et al., 2007) or by paracrine effects on DC and other APC, even during thymic development, remains to be determined.

In which sites do $nT_H21$ cells originate? Our results are consistent with both thymic and peripheral origins in a similar manner to that described for naturally-activated FoxP3 $T_{REG}$ cells. Natural $T_{REG}$ can arise as a direct result of thymic selection (referred to as thymic $T_{REG}$ and most recently as triple$^{hi}$ FoxP3 $T_{REG}$) or by the induction of naïve cells in the periphery ($pT_{REG}$) (Wyss et al., 2016; Yadav et al., 2013). It is quite unlikely that thymic $nT_H21$ derive from the peripheral pool because thymic $nT_H21$ cells rarely exceed 0.4% of $CD4^+$ $CD8^-$ thymocytes despite 5- to 10-fold higher frequencies in the periphery that accrue as normal mice age and 100-fold higher frequencies in FoxP3-deficient mice. Moreover, $nT_H21$ adoptively transferred into the periphery of T cell-deficient mice do not access thymi despite having appreciable peripheral frequencies (data not shown). Conversely, peripheral $nT_H21$ cells were found in normal frequencies in neonatally thymectomized mice (data not shown). Moreover, we found that peripheral $nT_H21$ cells are greatly reduced by antibiotic treatment while thymic frequencies were not affected. Our results are thus consistent with thymic and peripheral origins of $nT_H21$ cells with the former being insulated from peripheral stimuli until they merge with those induced in the periphery.

The diametrically opposed effects of AIRE provide further insights into differential modes of thymic and peripheral $nT_H21$ cell induction. Recent findings showed that AIRE channels a significant fraction of most highly self-reactive T cell clones that escape negative thymic selection into a $T_{REG}$ lineage (Kieback et al., 2016; Malchow et al., 2016; Malhotra and Jenkins, 2016). Similarly, we found that thymic development of $nT_H21$ is dependent on AIRE in a dose-dependent manner. Our results thus support an integral role for AIRE-dependent self-antigens in the positive thymic selection of $nT_H21$, similarly to that described for thymic $nT_{REG}$ cells.

In contrast, we found that mice deficient in AIRE had substantial increases in peripheral $nT_H21$ cells despite their reduction in the thymus. A deficiency in AIRE mistakenly diverts highly self-reactive thymocytes from $T_{REG}$ cells to aggressive self-reactive conventional T cells that “go rogue” upon escape into the periphery (Kieback et al., 2016; Malchow et al., 2016; Malhotra and Jenkins, 2016). Still to be determined is whether this increase can be attributed to the selective peripheral expansion of already activated $nT_H21$ cells surviving thymic selection or by naïve self-reactive thymic emigrants freshly activated on encounter with new antigens and/or microbial cues in the periphery.

Other features shared by $nT_H21$ and $nT_{REG}$ cells are their emergence in early post-natal life in frequencies that exceed other naturally activated thymic and peripheral $CD4^+$ T cell populations. Consistent with positive selection and activation by strong avidity TCR/self-p/MHC signals, thymic $nT_H21$ and $nT_{REG}$ cells both express high levels of Nur77 and are heavily dependent on AIRE. TCR transgenic mice have been instrumental in establishing the importance of strong TCR/self-p/MHC reactivity in the preferential positive selection of $T_{REG}$ cells (Hsieh et al., 2004; Kieback et al., 2016; Malchow et al., 2016). In a similar manner, the marked elevations of thymic and peripheral $nT_H21$ cells that we found in KRN TCR transgenic K/BXN mice, whose development of pathogenic $T_{FH}$ is strictly dependent on the NOD $H2^{g7}$ MHC, suggests that an alternative outcome of selection for strong TCR/self-p/MHC reactivity is the enhanced positive selection of potentially dangerous $nT_H21$ cells. We also found that the absence of FoxP3 results in substantial increases in peripheral $nT_H21$, findings consistent with reports showing that $IL21^+$ T cells are increased in scurfy mice (Iwamoto et al., 2014; Wing et al., 2014). Thus, $nT_H21$ and $nT_{REG}$ cells may develop self-reactivity through similar selection processes and at comparable frequencies but with opposing regulatory and autoimmune capabilities.

Our identification of $nT_H21$ cells that arise in neonatal life may shed light on the origins of $T_{FH}$ and related IL21-expressing extrafollicular $T_H$ cell populations that contribute to autoimmune diseases. A feature shared by *Aire*$^{-/-}$, *Foxp3*$^{-/-}$ and K/BxN mice is substantial increases in activated peripheral $IL21^+$ CD4 T cells. Among these $IL21^+$ populations, the largest increase was consistently seen in $nT_H21$ rather than mature $T_{FH}$. This points to the probable importance of $nT_H21$ as the stage at which failure to control self-reactivity leads to the development of autoimmune disease. Thus, failure to limit the activation, expansion and further maturation of this intrinsically self-reactive population may underlie autoimmune disorders in which IL21, $T_{FH,}$ and autoantibodies are important pathogenic drivers.

## EXPERIMENTAL PROCEDURES

### Generation of IL21-VFP reporter mice

The bicistronic IL21-VFP knock-in allele (*Il21*$^{tm1.1Hm}$) was generated in C57BL/6N ES cells by Ozgene Pty. Ltd. (Bentley WA) under the direction of HCM part of a contract with NIAID, NIH. Both hemizygous and homozygous *IL21-VFP* mice were used with zygosity consistent within each experiment. B6.IL21-VFP mice are available on request (D.C.R., H.C.M.) See Supplemental Experimental Procedures for reporter design and genotyping information.

### Mice

All mouse work was conducted according to national guidelines and approved by the Institutional Animal Care and Use Committee of The Jackson Laboratory (AUS 01022). All animals were maintained in a specific pathogen-free mouse colony and experiments were performed using C57BL/6-background mice except where otherwise indicated. Experiments involving the IL21-VFP reporter were either hemizygous and homozygous for *IL21-VFP* with zygosity consistent within each experiment. Cohorts were age matched within one wk of age with similar numbers of male and female mice in each experiment unless otherwise

noted. Ages of mice were between two and thirteen weeks of age. Details on the mouse strains, crosses, genotyping and breeding are described in Supplemental Experimental Procedures.

## Flow Cytometry

Analytical flow cytometry was performed by established procedures after FMO gating of viable cells (McPhee et al., 2013) using antibodies listed in Supplemental Experimental Procedures. Samples were run on a four-laser/13-color BD LSRII cytometer (BD Biosciences) and analyzed with FlowJo software version 8 or 9 (Tree Star). For spectral discrimination of VFP and GFP, a 510/20 filter was used in combination with the 505LP filter for detection of GFP in the FITC channel, and a 542/27 filter was used in combination with a 525L filter for detection of VFP/YFP in the PE channel. In each experiment, compensation and gating were based on cells single positive for GFP or VFP.

## T Cell Purification

For RNAseq splenic $CD4^+$ T cells were isolated using Milltenyi streptavidin microbeads (Milltenyil; BD Bioscience) coupled with CD11b, CD11c, B220 and CD8 antibodies followed by a pass through the autoMACS pro separator (Milltenyi) according to the manufacturer's protocols. Isolation of N, ACT and $nT_H21$ cells for RNAseq was then performed by FACS based on VFP, anti-CD4 and anti-ICOS detection using a FACSAria (BD Biosciences).

## RNAseq

Total RNA from purified N, ACT and $nT_H21$ spleen cell pools were extracted with Qiagen RNeasy Mini Kits (Qiagen, Hilden, Germany). Poly-A-enriched mRNA was reverse transcribed and amplified using the NuGEN Ovation Kit (NuGEN, San Carlos, CA, USA). Paired-end cDNA was sequenced with an Illumina MiSeq at 106 base pair length (Illumina, San Diego, CA, USA). Reads were checked with FASTX-Toolkit (http://hannonlab.cshl.edu/fastx_toolkit), trimmed with Trimmomatic, and aligned to the GRCm38.73 assembly transcriptome with Bowtie. Transcript expression levels were estimated in transcripts per million (TPM) using RSEM (Li and Dewey, 2011). Differential expression analysis across the sorted populations was conducted with EBSeq (Leng et al., 2013). Detailed analytical procedures are described in Supplemental Experimental Procedures

## Immunization and cell culture

Mice were immunized intraperitoneally with 200μL Dinitrophenyl conjugated keyhole limpet hemocyanin (DNP-KLH) emulsified in complete Freund's adjuvant and analyzed 7–11 days after immunization. For in vitro stimulation, total splenocytes from naïve B6.IL21-VFP mice depleted of red blood cells by exposure to ACK buffer were cultured in 6 well plates with 5 μg/ml of anti-CD3 and 1 μg/ml of anti-CD28 for 24 or 36hrs in 5% FBS-supplemented DMEM. Cells were then stained and sorted for being $CD4^+VFP^-$ and $CD4^+VFP^+$. Gene expression analysis by RT-qPCR and serum cytokine analysis after in vitro stimulation are described in Supplemental Experimental Procedures.

### Immunohistochemistry

Detailed protocols and reagents are described in Supplemental Experimental Procedures.

### Statistical analyses

Statistical analyses were performed in GraphPad Prism v6 using non-parametric tests that do not assume a normal distribution. The Mann-Whitney U test was used for two-way comparisons and Kruskal-Wallis was used for multigroup comparisons. “n” refers to the number of individual mice sampled per cohort with Mean ± SD indicated. Comparisons of $p \leq 0.05$ were considered to be significant. All experiments were repeated at least twice to ensure reproducibility and reliable interpretations. RNAseq analysis is described under “RNAseq” and Supplemental Experimental Procedures.

## Supplementary Material

Refer to Web version on PubMed Central for supplementary material.

## Acknowledgments

We thank J. Ward (Global VetPathology) for assistance with IHC images; D. Serreze (The Jackson Laboratory) for manuscript review; Gene Expression Service (The Jackson Laboratory) for RNA sequencing; John Wilson and Porcia Mandanhar for technical assistance. Supported in part by the Alliance for Lupus Research (D.C.R.), New England Biolabs (D.C.R), The Gina M. Finzi memorial student summer fellowship from the Lupus Foundation of America (E.A.M.), The Jackson Laboratory summer student program (S.L.K.), the Intramural Research Program of the NIH, NIAID (H.C.M., S.J., and H.W.) and The Pyewacket Foundation (X.W. and G.W.C.).

## References

Akiba H, Takeda K, Kojima Y, Usui Y, Harada N, Yamazaki T, Ma J, Tezuka K, Yagita H, Okumura K. The role of ICOS in the CXCR5+ follicular B helper T cell maintenance in vivo. J Immunol. 2005; 175:2340–2348. [PubMed: 16081804]

Barnett LG, Simkins HM, Barnett BE, Korn LL, Johnson AL, Wherry EJ, Wu GF, Laufer TM. B cell antigen presentation in the initiation of follicular helper T cell and germinal center differentiation. Journal of immunology. 2014; 192:3607–3617.

Block KE, Huang H. The cellular source and target of IL-21 in K/BxN autoimmune arthritis. J Immunol. 2013; 191:2948–2955. [PubMed: 23960240]

Block KE, Zheng Z, Dent AL, Kee BL, Huang H. Gut Microbiota Regulates K/BxN Autoimmune Arthritis through Follicular Helper T but Not Th17 Cells. J Immunol. 2016; 196:1550–1557. [PubMed: 26783341]

Bubier JA, Sproule TJ, Foreman O, Spolski R, Shaffer DJ, Morse HC 3rd, Leonard WJ, Roopenian DC. A critical role for IL-21 receptor signaling in the pathogenesis of systemic lupus erythematosus in BXSB-Yaa mice. Proceedings of the National Academy of Sciences of the United States of America. 2009; 106:1518–1523. [PubMed: 19164519]

Cai G, Nie X, Zhang W, Wu B, Lin J, Wang H, Jiang C, Shen Q. A regulatory role for IL-10 receptor signaling in development and B cell help of T follicular helper cells in mice. J Immunol. 2012; 189:1294–1302. [PubMed: 22753938]

Carpio VH, Opata MM, Montanez ME, Banerjee PP, Dent AL, Stephens R. IFN-gamma and IL-21 Double Producing T Cells Are Bcl6-Independent and Survive into the Memory Phase in Plasmodium chabaudi Infection. PloS one. 2015; 10:e0144654. [PubMed: 26646149]

Choi YS, Gullicksrud JA, Xing S, Zeng Z, Shan Q, Li F, Love PE, Peng W, Xue HH, Crotty S. LEF-1 and TCF-1 orchestrate T(FH) differentiation by regulating differentiation circuits upstream of the transcriptional repressor Bcl6. Nat Immunol. 2015; 16:980–990. [PubMed: 26214741]

Choi YS, Kageyama R, Eto D, Escobar TC, Johnston RJ, Monticelli L, Lao C, Crotty S. ICOS receptor instructs T follicular helper cell versus effector cell differentiation via induction of the transcriptional repressor Bcl6. Immunity. 2011; 34:932–946. [PubMed: 21636296]

Coquet JM, Kyparissoudis K, Pellicci DG, Besra G, Berzins SP, Smyth MJ, Godfrey DI. IL-21 is produced by NKT cells and modulates NKT cell activation and cytokine production. J Immunol. 2007; 178:2827–2834. [PubMed: 17312126]

Crotty S. T follicular helper cell differentiation, function, and roles in disease. Immunity. 2014; 41:529–542. [PubMed: 25367570]

Cucak H, Yrlid U, Reizis B, Kalinke U, Johansson-Lindbom B. Type I interferon signaling in dendritic cells stimulates the development of lymph-node-resident T follicular helper cells. Immunity. 2009; 31:491–501. [PubMed: 19733096]

Davis MR, Zhu Z, Hansen DM, Bai Q, Fang Y. The role of IL-21 in immunity and cancer. Cancer Lett. 2015; 358:107–114. [PubMed: 25575696]

Eto D, Lao C, DiToro D, Barnett B, Escobar TC, Kageyama R, Yusuf I, Crotty S. IL-21 and IL-6 are critical for different aspects of B cell immunity and redundantly induce optimal follicular helper CD4 T cell (Tfh) differentiation. PloS one. 2011; 6:e17739. [PubMed: 21423809]

Ettinger R, Kuchen S, Lipsky PE. The role of IL-21 in regulating B-cell function in health and disease. Immunological reviews. 2008; 223:60–86. [PubMed: 18613830]

Goenka R, Barnett LG, Silver JS, O'Neill PJ, Hunter CA, Cancro MP, Laufer TM. Cutting edge: dendritic cell-restricted antigen presentation initiates the follicular helper T cell program but cannot complete ultimate effector differentiation. Journal of immunology. 2011; 187:1091–1095.

Hogquist KA, Jameson SC. The self-obsession of T cells: how TCR signaling thresholds affect fate 'decisions' and effector function. Nature immunology. 2014; 15:815–823. [PubMed: 25137456]

Hsieh CS, Liang Y, Tyznik AJ, Self SG, Liggitt D, Rudensky AY. Recognition of the peripheral self by naturally arising CD25+ CD4+ T cell receptors. Immunity. 2004; 21:267–277. [PubMed: 15308106]

Iwamoto T, Suto A, Tanaka S, Takatori H, Suzuki K, Iwamoto I, Nakajima H. Interleukin-21-producing c-Maf-expressing CD4+ T cells induce effector CD8+ T cells and enhance autoimmune inflammation in scurfy mice. Arthritis & rheumatology (Hoboken, NJ). 2014; 66:2079–2090.

Jain S, Chen J, Nicolae A, Wang H, Shin DM, Adkins EB, Sproule TJ, Leeth CM, Sakai T, Kovalchuk AL, et al. IL-21-driven neoplasms in SJL mice mimic some key features of human angioimmunoblastic T-cell lymphoma. The American Journal of Pathology. 2015; 185:3102–3114. [PubMed: 26363366]

Jang E, Cho SH, Park H, Paik DJ, Kim JM, Youn J. A positive feedback loop of IL-21 signaling provoked by homeostatic CD4+CD25- T cell expansion is essential for the development of arthritis in autoimmune K/BxN mice. J Immunol. 2009; 182:4649–4656. [PubMed: 19342640]

Jenkinson WE, McCarthy NI, Dutton EE, Cowan JE, Parnell SM, White AJ, Anderson G. Natural Th17 cells are critically regulated by functional medullary thymic microenvironments. Journal of autoimmunity. 2015; 63:13–22. [PubMed: 26143957]

Johnston RJ, Poholek AC, DiToro D, Yusuf I, Eto D, Barnett B, Dent AL, Craft J, Crotty S. Bcl6 and Blimp-1 are reciprocal and antagonistic regulators of T follicular helper cell differentiation. Science (New York, NY). 2009; 325:1006–1010.

Kieback E, Hilgenberg E, Stervbo U, Lampropoulou V, Shen P, Bunse M, Jaimes Y, Boudinot P, Radbruch A, Klemm U, et al. Thymus-Derived Regulatory T Cells Are Positively Selected on Natural Self-Antigen through Cognate Interactions of High Functional Avidity. Immunity. 2016; 44:1114–1126. [PubMed: 27192577]

Korganow AS, Ji H, Mangialaio S, Duchatelle V, Pelanda R, Martin T, Degott C, Kikutani H, Rajewsky K, Pasquali JL, et al. From systemic T cell self-reactivity to organ-specific autoimmune disease via immunoglobulins. Immunity. 1999; 10:451–461. [PubMed: 10229188]

Korn T, Bettelli E, Oukka M, Kuchroo VK. IL-17 and Th17 Cells. Annual review of immunology. 2009; 27:485–517.

Kouskoff V, Korganow AS, Duchatelle V, Degott C, Benoist C, Mathis D. Organ-specific disease provoked by systemic autoimmunity. Cell. 1996; 87:811–822. [PubMed: 8945509]

Lee SK, Rigby RJ, Zotos D, Tsai LM, Kawamoto S, Marshall JL, Ramiscal RR, Chan TD, Gatto D, Brink R, et al. B cell priming for extrafollicular antibody responses requires Bcl-6 expression by T cells. The Journal of experimental medicine. 2011; 208:1377–1388. [PubMed: 21708925]

Leng N, Dawson JA, Thomson JA, Ruotti V, Rissman AI, Smits BM, Haag JD, Gould MN, Stewart RM, Kendziorski C, et al. EBSeq: an empirical Bayes hierarchical model for inference in RNA-seq experiments RSEM: accurate transcript quantification from RNA-Seq data with or without a reference genome. Ultrafast and memory-efficient alignment of short DNA sequences to the human genome. Bioinformatics. 2013; 29:1035–1043. doi:1010.1093/bioinformatics/btt1087. Epub 2013 Feb 1021. [PubMed: 23428641]

Li B, Dewey CN. RSEM: accurate transcript quantification from RNA-Seq data with or without a reference genome. BMC Bioinformatics. 2011; 12:323. [PubMed: 21816040]

Liston A, Lesage S, Wilson J, Peltonen L, Goodnow CC. Aire regulates negative selection of organ-specific T cells. Nat Immunol. 2003; 4:350–354. [PubMed: 12612579]

Liu X, Chen X, Zhong B, Wang A, Wang X, Chu F, Nurieva RI, Yan X, Chen P, van der Flier LG, et al. Transcription factor achaete-scute homologue 2 initiates follicular T-helper-cell development. Nature. 2014; 507:513–518. [PubMed: 24463518]

Liu X, Yan X, Zhong B, Nurieva RI, Wang A, Wang X, Martin-Orozco N, Wang Y, Chang SH, Esplugues E, et al. Bcl6 expression specifies the T follicular helper cell program in vivo. The Journal of experimental medicine. 2012; 209:1841–1852. S1841–1824. [PubMed: 22987803]

Malchow S, Leventhal DS, Lee V, Nishi S, Socci ND, Savage PA. Aire Enforces Immune Tolerance by Directing Autoreactive T Cells into the Regulatory T Cell Lineage. Immunity. 2016; 44:1102–1113. [PubMed: 27130899]

Malhotra D, Jenkins MK. Regulatory T Cells: A Crisis Averted. Immunity. 2016; 44:1079–1081. [PubMed: 27192571]

Marks BR, Nowyhed HN, Choi JY, Poholek AC, Odegard JM, Flavell RA, Craft J. Thymic self-reactivity selects natural interleukin 17-producing T cells that can regulate peripheral inflammation. Nat Immunol. 2009; 10:1125–1132. [PubMed: 19734905]

McGuire HM, Vogelzang A, Ma CS, Hughes WE, Silveira PA, Tangye SG, Christ D, Fulcher D, Falcone M, King C. A subset of interleukin-21+ chemokine receptor CCR9+ T helper cells target accessory organs of the digestive system in autoimmunity. Immunity. 2011; 34:602–615. [PubMed: 21511186]

McPhee CG, Bubier JA, Sproule TJ, Park G, Steinbuck MP, Schott WH, Christianson GJ, Morse HC 3rd, Roopenian DC. IL-21 is a double-edged sword in the systemic lupus erythematosus-like disease of BXSB.Yaa mice. Journal of immunology. 2013; 191:4581–4588.

Moran AE, Hogquist KA. T-cell receptor affinity in thymic development. Immunology. 2012; 135:261–267. [PubMed: 22182461]

Nakayamada S, Poholek AC, Lu KT, Takahashi H, Kato M, Iwata S, Hirahara K, Cannons JL, Schwartzberg PL, Vahedi G, et al. Type I IFN induces binding of STAT1 to Bcl6: divergent roles of STAT family transcription factors in the T follicular helper cell genetic program. Journal of immunology. 2014; 192:2156–2166.

Nurieva R, Yang XO, Martinez G, Zhang Y, Panopoulos AD, Ma L, Schluns K, Tian Q, Watowich SS, Jetten AM, Dong C. Essential autocrine regulation by IL-21 in the generation of inflammatory T cells. Nature. 2007; 448:480–483. [PubMed: 17581589]

Odegard JM, Marks BR, DiPlacido LD, Poholek AC, Kono DH, Dong C, Flavell RA, Craft J. ICOS-dependent extrafollicular helper T cells elicit IgG production via IL-21 in systemic autoimmunity. The Journal of experimental medicine. 2008; 205:2873–2886. [PubMed: 18981236]

Qiao Y, Zhu L, Sofi H, Lapinski PE, Horai R, Mueller K, Stritesky GL, He X, Teh HS, Wiest DL, et al. Development of promyelocytic leukemia zinc finger-expressing innate CD4 T cells requires stronger T-cell receptor signals than conventional CD4 T cells. Proceedings of the National Academy of Sciences of the United States of America. 2012; 109:16264–16269. [PubMed: 22988097]

Ramsdell F, Ziegler SF. FOXP3 and scurfy: how it all began. Nature reviews Immunology. 2014; 14:343–349.

Ray JP, Marshall HD, Laidlaw BJ, Staron MM, Kaech SM, Craft J. Transcription factor STAT3 and type I interferons are corepressive insulators for differentiation of follicular helper and T helper 1 cells. Immunity. 2014; 40:367–377. [PubMed: 24631156]

Spolski R, Leonard WJ. Interleukin-21: a double-edged sword with therapeutic potential. Nat Rev Drug Discov. 2014; 13:379–395. [PubMed: 24751819]

Stone EL, Pepper M, Katayama CD, Kerdiles YM, Lai CY, Emslie E, Lin YC, Yang E, Goldrath AW, Li MO, et al. ICOS Coreceptor Signaling Inactivates the Transcription Factor FOXO1 to Promote Tfh Cell Differentiation. Immunity. 2015; 42:239–251. [PubMed: 25692700]

Teng F, Klinger CN, Felix KM, Bradley CP, Wu E, Tran NL, Umesaki Y, Wu HJ. Gut Microbiota Drive Autoimmune Arthritis by Promoting Differentiation and Migration of Peyer's Patch T Follicular Helper Cells. Immunity. 2016; 44:875–888. [PubMed: 27096318]

Wang H, Geng J, Wen X, Bi E, Kossenkov AV, Wolf AI, Tas J, Choi YS, Takata H, Day TJ, et al. The transcription factor Foxp1 is a critical negative regulator of the differentiation of follicular helper T cells. Nat Immunol. 2014; 15:667–675. [PubMed: 24859450]

Weber JP, Fuhrmann F, Feist RK, Lahmann A, Al Baz MS, Gentz LJ, Vu Van D, Mages HW, Haftmann C, Riedel R, et al. ICOS maintains the T follicular helper cell phenotype by down-regulating Kruppel-like factor 2. The Journal of Experimental Medicine. 2015; 212:217–233. [PubMed: 25646266]

Wei L, Laurence A, Elias KM, O'Shea JJ. IL-21 is produced by Th17 cells and drives IL-17 production in a STAT3-dependent manner. J Biol Chem. 2007; 282:34605–34610. [PubMed: 17884812]

Wing JB, Ise W, Kurosaki T, Sakaguchi S. Regulatory T cells control antigen-specific expansion of Tfh cell number and humoral immune responses via the coreceptor CTLA-4. Immunity. 2014; 41:1013–1025. [PubMed: 25526312]

Wu HJ, Ivanov II, Darce J, Hattori K, Shima T, Umesaki Y, Littman DR, Benoist C, Mathis D. Gut-residing segmented filamentous bacteria drive autoimmune arthritis via T helper 17 cells. Immunity. 2010; 32:815–827. [PubMed: 20620945]

Wyss L, Stadinski BD, King CG, Schallenberg S, McCarthy NI, Lee JY, Kretschmer K, Terracciano LM, Anderson G, Surh CD, et al. Affinity for self antigen selects Treg cells with distinct functional properties. Nat Immunol. 2016; 17:1093–1101. [PubMed: 27478940]

Xu L, Cao Y, Xie Z, Huang Q, Bai Q, Yang X, He R, Hao Y, Wang H, Zhao T, et al. The transcription factor TCF-1 initiates the differentiation of T(FH) cells during acute viral infection. Nat Immunol. 2015; 16:991–999. [PubMed: 26214740]

Yadav M, Stephan S, Bluestone JA. Peripherally induced tregs - role in immune homeostasis and autoimmunity. Front Immunol. 2013; 4:232. [PubMed: 23966994]

Yang S, Fujikado N, Kolodin D, Benoist C, Mathis D. Immune tolerance. Regulatory T cells generated early in life play a distinct role in maintaining self-tolerance. Science (New York, NY). 2015; 348:589–594.

Yu D, Rao S, Tsai LM, Lee SK, He Y, Sutcliffe EL, Srivastava M, Linterman M, Zheng L, Simpson N, et al. The transcriptional repressor Bcl-6 directs T follicular helper cell lineage commitment. Immunity. 2009; 31:457–468. [PubMed: 19631565]

Yusuf I, Kageyama R, Monticelli L, Johnston RJ, Ditoro D, Hansen K, Barnett B, Crotty S. Germinal center T follicular helper cell IL-4 production is dependent on signaling lymphocytic activation molecule receptor (CD150). J Immunol. 2010; 185:190–202. [PubMed: 20525889]

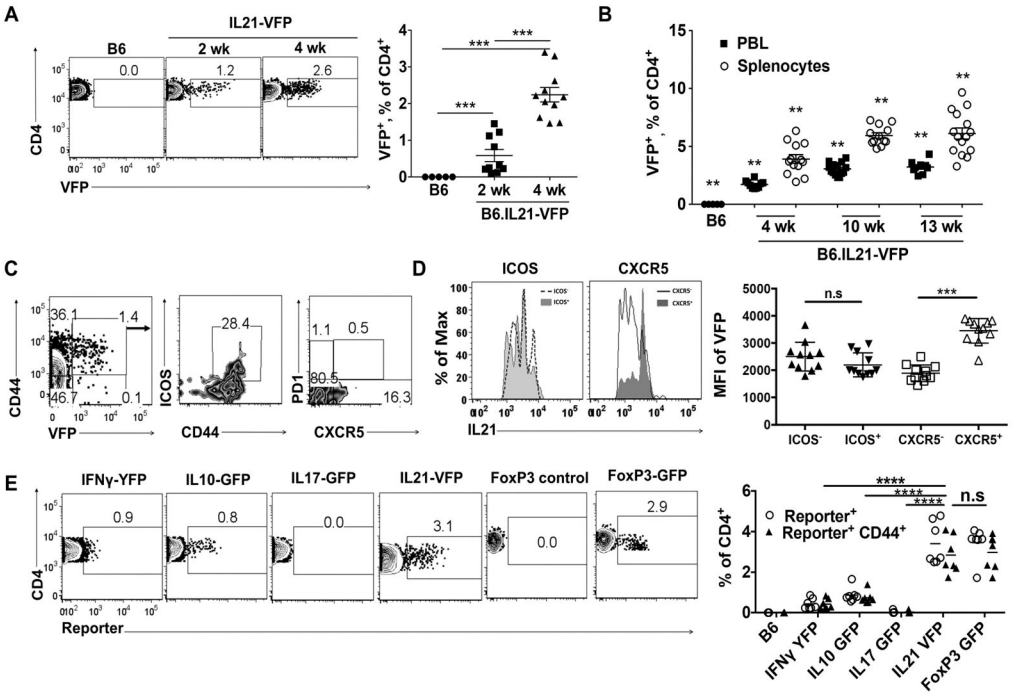


**Figure 1. IL21-expressing CD4 T cells are the major population of activated CD4 T cells that arises in young naïve mice**

**(A)** Example FACS plots of splenic VFP$^+$ CD4$^+$ T cells from 2 and 4 wk old naïve IL21-VFP and reporter-negative control mice (B6:n=5; 2 wk:n=10; 4 wk: n=11). (**B**) Summary of splenic and PBL VFP$^+$ CD4 T cell frequencies from naïve IL21-VFP mice of indicated ages. Increase over time is significant by P ≤0.02 (Kruskal-Wallis) (B6:n=5; 4wk:n=10,12; 10wk:n=13,14; 13wk: n=9,15) **(C)** Representative analyses of CD44, ICOS, CXCR5 and PD1 expression by VFP$^+$ splenic CD4$^+$ T cells from 4 wk old naïve IL21-VFP mice (n=15). **(D)** Left: Representative MFI of VFP in CD4 T cells based on ICOS and CXCR5 expression. Right: combined data (n=11). **(E)** Left: Representative FACS plots comparing reporter expression of CD4 T cells from splenocytes of 4 to 6 wk old IL21-VFP, IL17-GFP, IL10-GFP, IFNγ-YFP and FoxP3-GFP heterozygous reporter mice on a B6 background. Right: Summarized percentages of reporter-positive CD4 T cells (circle) and gated as CD44$^{hi}$ (triangle) (B6:n=4; IFNγ:n=7; IL10:n=8; IL17:n=4; IL21:n=7; FoxP3:n=6). n, number of mice/cohort. Representative of at least four independent experiments. ** P ≤0.01, *** P≤0.001; *** P ≤0.0001; n.s, not significant. Mean ± SD is indicated. See also Figure S1 and S2.

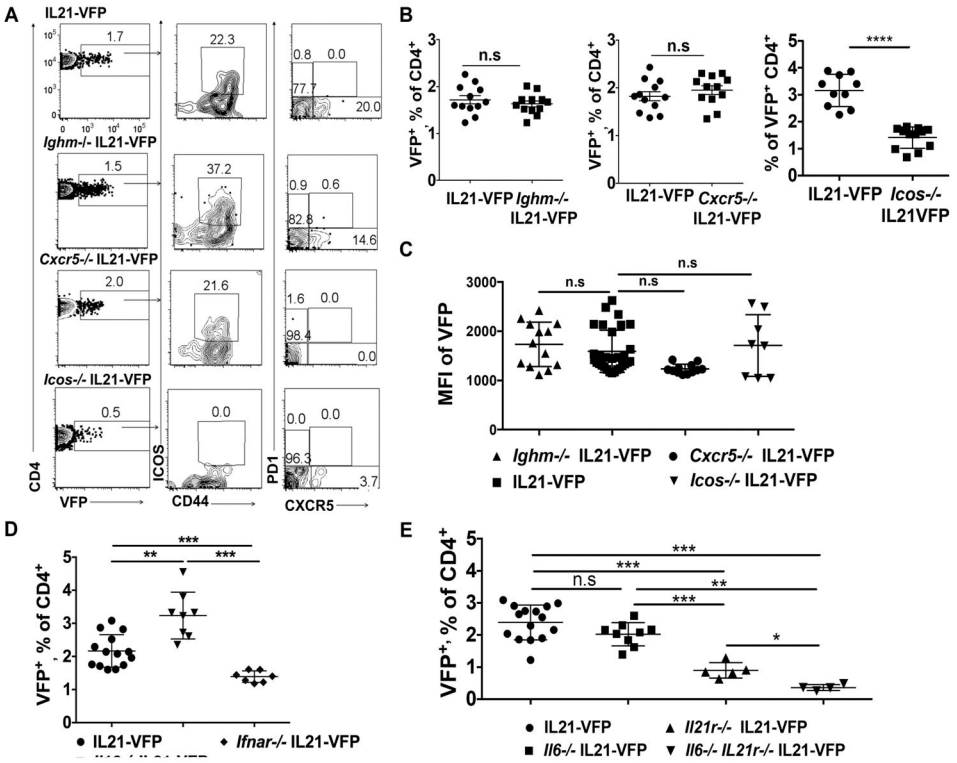


**Figure 2. Cellular, chemokine and cytokine requirements of IL21$^+$ CD4 T cells**

**(A)** FACS plots of VFP$^+$CD4 T cells in PBL from 4 wk old WT, *Ighm*$^{-/-}$, *Cxcr5*$^{-/-}$ and *Icos*$^{-/-}$ IL21-VFP mice. Also shows co-expression of CD44, ICOS, CXCR5 and PD1 (n=12). **(B)** Frequencies of VFP$^+$CD4 T cells in PBL from *Ighm*$^{-/-}$, *Cxcr5*$^{-/-}$, and *Icos*$^{-/-}$ and WT IL21- VFP mice (n=12). (**C**) MFI of VFP by CD4$^+$ T cells; pooled data from PBL of 4 wk old *Ighm*$^{-/-}$ (n=13), WT (n=28) *Cxcr5*$^{-/-}$ (n=12), *and Icos*$^{-/-}$ (n=8) IL21-VFP mice. (**D**) Frequencies of VFP$^+$ CD4 T cells in 5–6 wk old WT (n=14), *Il10*$^{-/-}$ IL21-VFP (n=8) and *Ifnar*$^{-/-}$ IL21-VFP mice. **(E)** Frequencies of VFP$^+$ CD4 T cells in 4–6 wk old WT (n=15), *Il6*$^{-/-}$ IL21-VFP (n=9), *Il21r*$^{-/-}$ IL21-VFP (n=5) and *Il6*$^{-/-}$ *Il21r*$^{-/-}$ (n=4) IL21-VFP mice. Representative of two to four independent experiments. * P ≤0.05; ** P ≤0.01; *** P≤0.001; n.s, not significant. Mean ± SD is indicated.

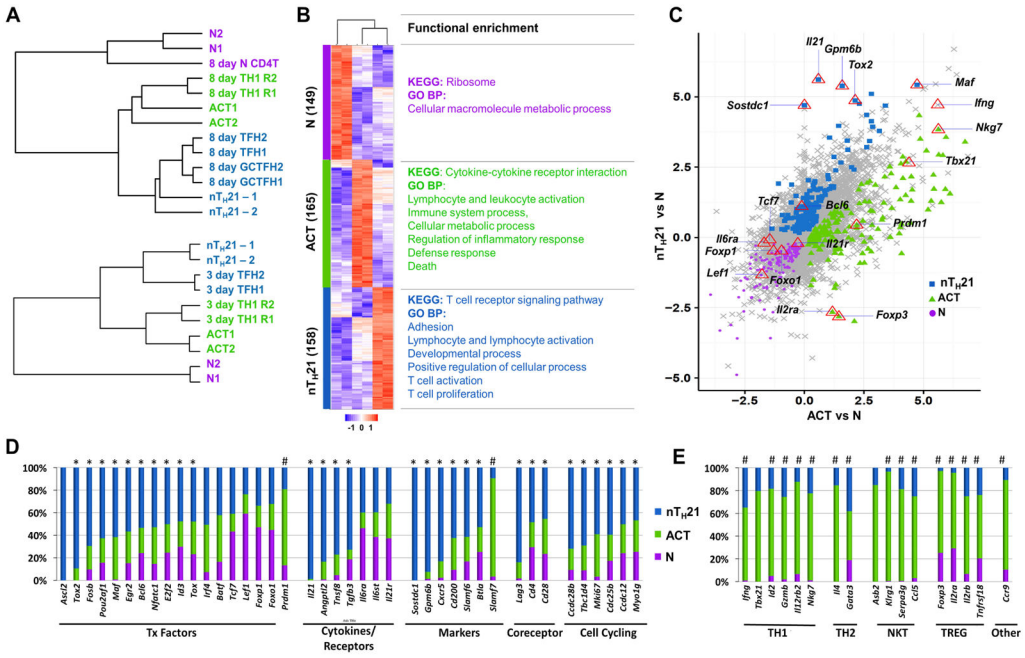


**Figure 3. RNAseq-based transcriptomic analysis of natural CD4 T cell populations**

**(A)** Comparisons of RNAseq profiles of N ($CD4^+$ $VFP^-$ $ICOS^{lo}$ $CD44^-$), ACT ($CD4^+$ $VFP^-ICOS^{hi}$ $CD44^+$) and $nT_H21$ ($CD4^+$ $VFP^+$ $ICOS^{hi/int}$ $CD44^+$) populations with microarray-based datasets with. Top: naïve, $T_H1$, $T_{FH}$ and GC $T_{FH}$ 8 days after an infection with LCMV (Yusuf et al., 2010). Bottom: RNAseq datasets of early $T_{FH}$ (IL-2Rα$^-$ $Blimp1^-$ $CXCR5^+$ $PD1^{lo}$) and early $T_H1$ (IL-2Rα $^+Blimp1^+CXCR5^-$) cells isolated 3 days after LCMV infection (Choi et al., 2015). **(B)** Heat map of the 471 genes that best discriminate N, ACT and $nT_H21$ with representative KEGG and GO BP functional enrichments ($P<1 \times 10^6$ and $1\times10^{-8}$, respectively. **(C)** Scatterplot of the $Log_2$ difference between each ACT sample and the N sample with the most discriminating N, ACT, and $nT_H21$ genes colored. Reference genes are indicated. (**D**) Expression patterns of N, ACT and $nT_H21$ for selected $T_{FH}$-associated genes. Data are shown as % representation of each transcript in the specified population. *, Selectively enriched in $nT_H21$; and #, transcripts significantly different at ≤0.05 by $nT_H21$ in comparison to N and ACT. (**E**) Expression patterns of genes of interest for $T_H1$, $T_H2$, NKT and $T_{REG}$. See also Figure S3, Table S1, Table S2 and Table S3.

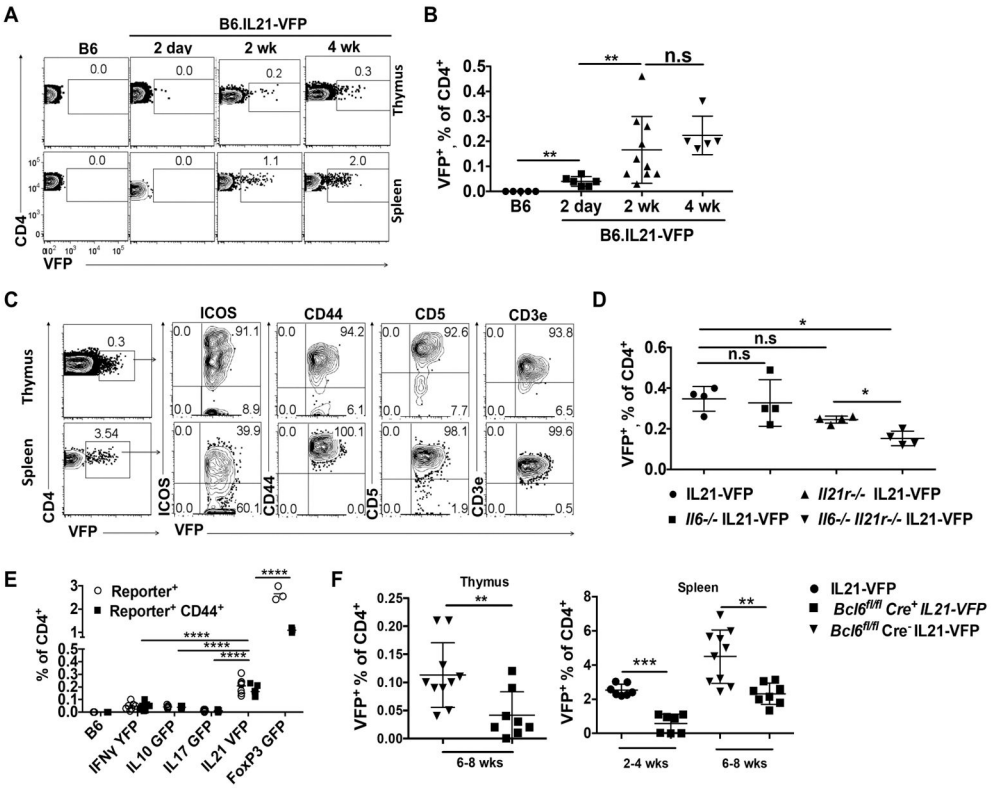


**Figure 4. IL6/IL21/BCL6-dependent nT$_H$21 cells are a major natural T-helper population to develop in the neonatal thymus**

(**A**) Representative thymic and splenic VFP expression patterns of CD4$^+$8$^-$ T cells from naïve IL21-VFP mice at varied ages. **(B)** Combined thymus data from A (see figure 1A for spleen) (B6:n=5; 2d:n=6; 2wk:n=10; 4wk:n=5) (**C**) Expression of ICOS, CD44, CD5 and CD3 by splenic and thymic nT$_H$21 (VFP$^+$ CD4$^+$) from 6 wk old mice (n=6). (**D**) Comparisons of thymic nT$_H$21 frequencies from WT, *Il6*$^{-/-}$, *Il21r*$^{-/-}$ and *Il6*$^{-/-}$*Il21r*$^{-/-}$ IL21-VFP mice (n=4). (**E**) 4–6 wk old heterozygous reporter mice were analyzed for thymic levels of IFN**γ**-YFP (n=6), IL10-GFP (n=5), IL17-GFP (n=5), IL21-VFP (n=6) and FoxP3-GFP (n=3). Total percentages of reporter-positive CD4$^+$8$^-$ T cells and of those that are also CD44$^+$ are shown. Statistics shown are comparing the CD44$^+$ subsets. (**F**) Frequency comparisons of thymic and splenic nT$_H$21 cells (VFP$^+$ CD4$^+$8$^-$) from IL21-VFP heterozygous *CD4-Cre*$^+$ *Bcl6*$^{fl/fl}$, *CD4-Cre*$^-$ *Bcl6*$^{fl/fl}$ and *Bcl6* WT mice at indicated ages (n=7–10). Representative of at least two independent experiments. * P ≤0.05, ** P ≤0.01, **** P≤0.0001; n.s, not significant. Mean ± SD is indicated. See also Figure S4.

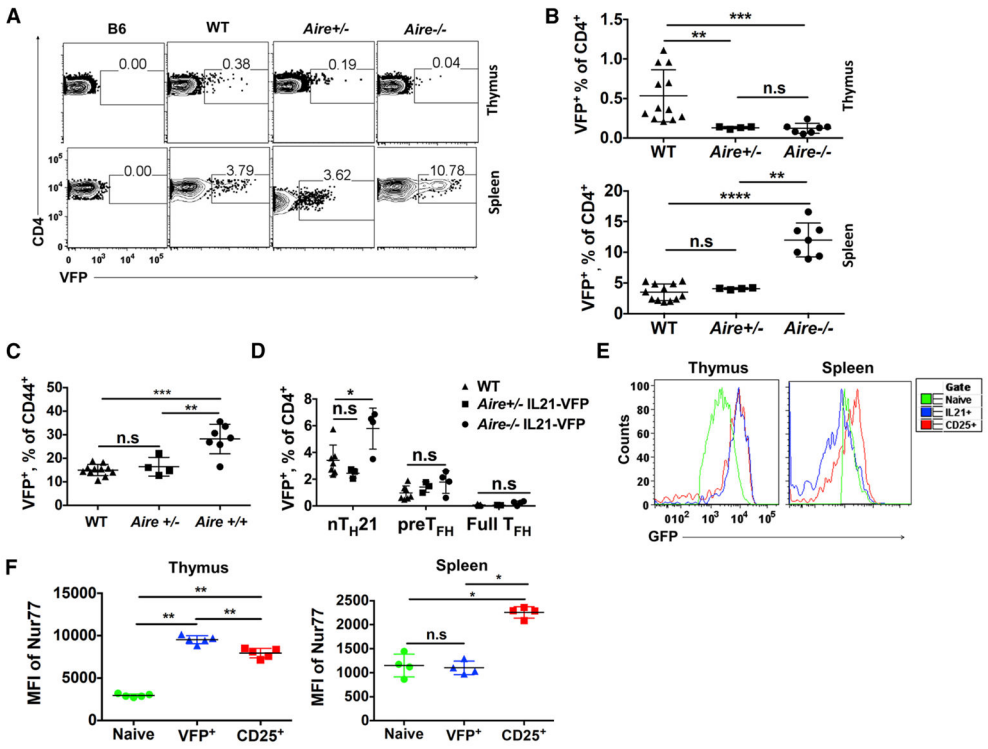


**Figure 5. Thymic but not peripheral nT$_H$21 cells require AIRE and express high levels of Nur77**

(**A–B**) Thymic and splenic VFP$^+$ CD4$^+$ T cell frequencies in 7 wk old WT (n=12), *Aire*$^{+/-}$ (n= 4) and *Aire*$^{-/-}$ (n=7) IL21-VFP mice. (**C**) Effect of *Aire* copy number on frequencies of CD44$^+$ splenic VFP$^+$ CD4$^+$ T cells (WT:n=11; *Aire*$^{+/-}$:n=4; *Aire*$^{-/-}$:n=7). (**D**) Splenic T$_H$ sources (CXCR5$^{lo}$ PD1$^-$ nT$_H$21; CXCR5$^{hi}$ PD1$^-$ pre-T$_{FH}$; CXCR5$^{hi}$ PD1$^+$ full T$_{FH}$) in WT (n=7), *Aire*$^{+/-}$ (n=4), *Aire*$^{-/-}$ (n=4) IL21-VFP mice. (**E**) Histograms of Nur77-GFP expression by thymic and splenic VFP$^+$, CD25$^+$ and naïve CD4$^+$ T cells (n=5). (**F**) Summary data from **E**. Representative of at least three independent experiments.* P ≤0.05, ** P ≤0.01, *** P ≤0.001, **** P≤0.0001; n.s, not significant. Mean ± SD is indicated.

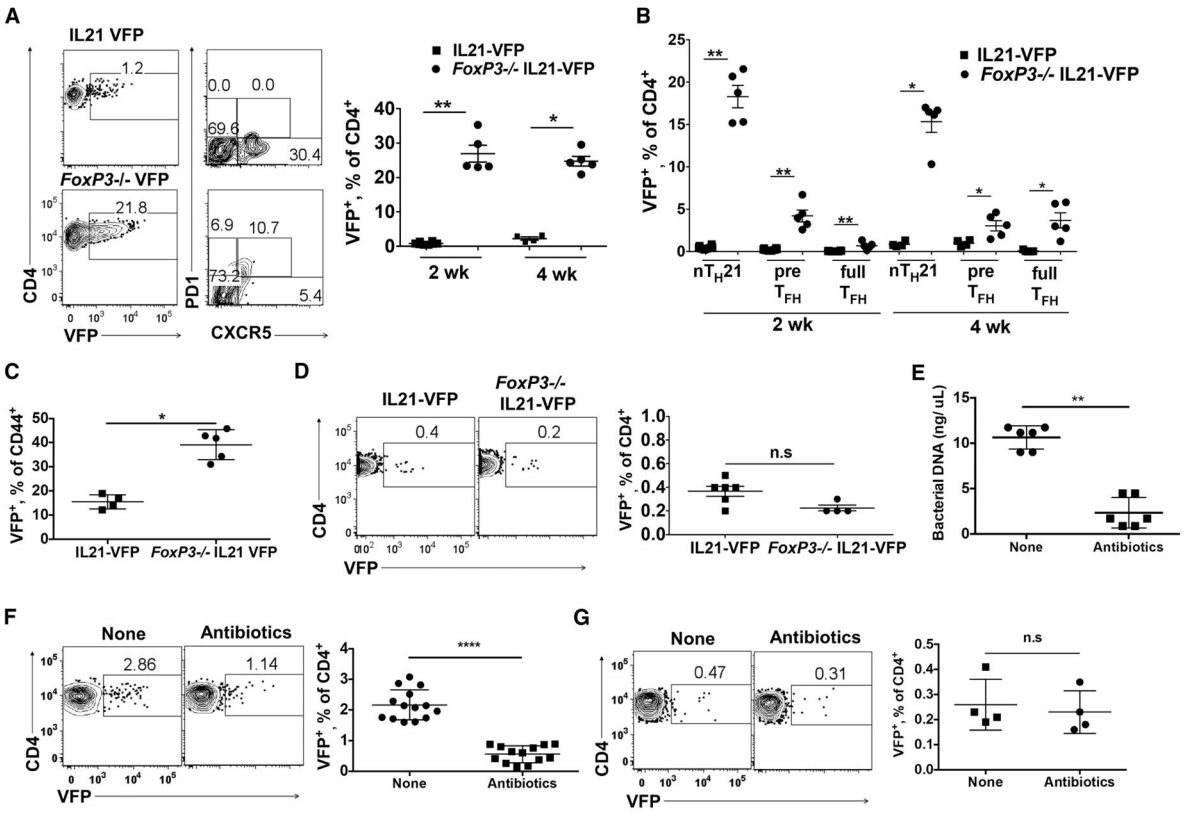


**Figure 6. FoxP3 and depletion of gut microbiota restrict the expansion and maturation of peripheral but not thymic $nT_H21$ cells**

(**A**) (Left); Representative plots of $VFP^+$ gated splenic T cells from 4 wk old *Foxp3*$^-$ (n=5) and WT (n=4) IL21-VFP male mice. (Right); Summary data showing 2 and 4 wks. (**B**) $VFP^+$ $CD4^+$ T cells from **A** at 2 weeks further distinguished as $nT_H21$, pre-$T_{FH}$ or full $T_{FH}$ cells (VFP:n=7; *FoxP3*:n=5). (**C**) Effects of *FoxP3*-deficiency on frequencies of activated $CD44^+$ splenic $VFP^+$ $CD4^+$ T cells (VFP:n=4; *FoxP3*:n=5). **(D)** Analysis of thymic $VFP^+$ $CD4^+8^-$ T cells from 4 wk old *Foxp3*$^-$ (n=4) and WT (n=5) IL21-VFP male mice. (**E**) Levels of fecal bacterial DNA detected by 16s RNA pyrosequencing from IL21-VFP mice untreated or treated for 4 wks with ampicillin/sulfatrim (n=6). (**F**) Analyses of splenic (n=13–14) and (**G**) thymic $VFP^+$ $CD4^+$ T cells (n=4) from antibiotic-treated and untreated mice. Representative of at least two independent experiments. * $P \leq 0.05$, ** $P \leq 0.01$, **** $P \leq 0.0001$; n.s, not significant. Mean ± SD is indicated.

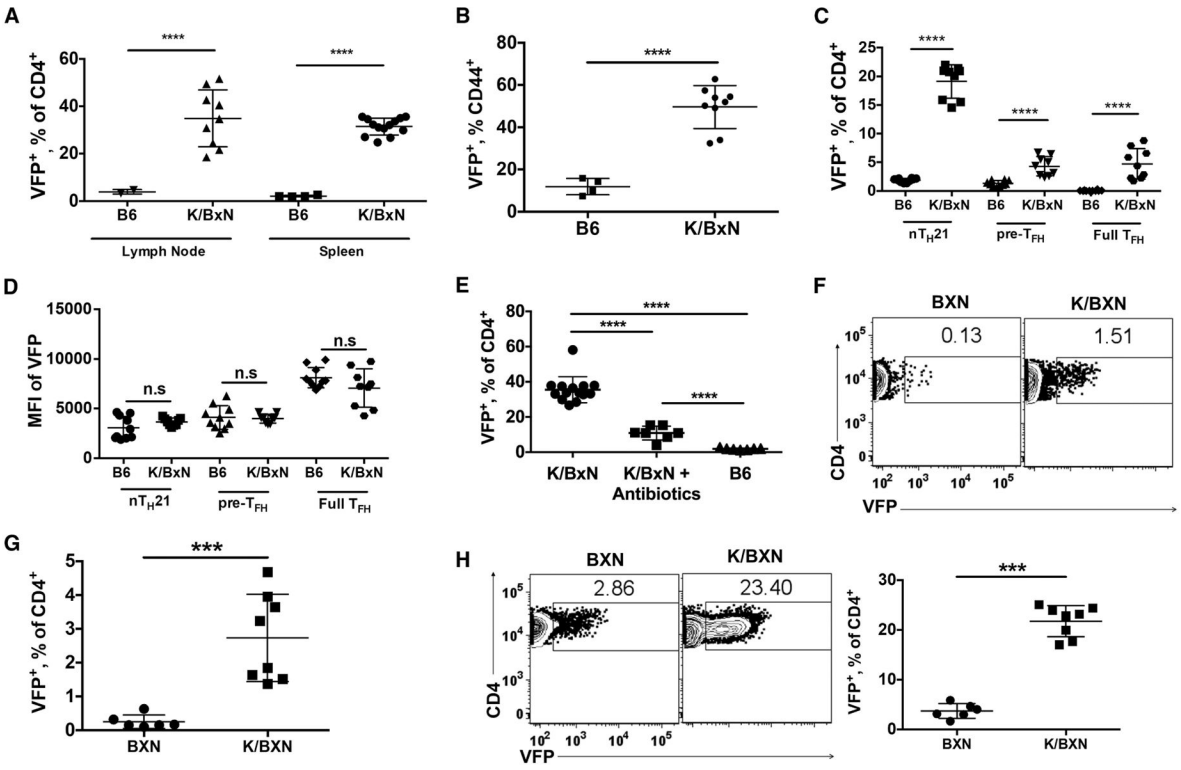


**Figure 7. Thymic and peripheral $nT_H21$ develop in unusually high frequencies in the IL21-dependent K/BXN model of autoimmune arthritis**

**(A)** Analysis of $VFP^+$ $CD4^+$ T cells from mesenteric lymph nodes (B6:n=2; K/BxN:n=9) and spleens (B6:n=4; K/BxN:n=13) of 10 wk old B6 IL21-VFP and K/BXN IL21-VFP mice. **(B)** Percentages of $VFP^+$ $CD44^{hi}$ splenic $CD4^+$ T cells of B6 (n=4) and K/BxN (n=9) IL21-VFP mice. (**C**) $VFP^+$ CD4 T cells further distinguished as $nT_H21$, pre-$T_{FH}$ or full $T_{FH}$ cells (n=9). (**D**) MFI of VFP expression by $CD4^+$ T cells from **C. (E)** Comparison of $CD4^+$ $VFP^+$ T cells from K/BxN (n=14), antibiotic treated K/BxN (n=7) and B6 (n=7) IL21-VFP mice. Analysis of $VFP^+$ $CD4^+$ T cells from **(F & G)** thymi and **(H)** spleens of 6 wk old BXN (n=6) and K/BXN (n=8) IL21-VFP mice. Representative of at least two independent experiments. *** $P \leq 0.001$, **** $P \leq 0.0001$; n.s, not significant. Mean ± SD is indicated.